Journal of Sensor Science and Technology
Vol. 29, No. 2 (2020) pp. 75-81
http://dx.doi.org/10.5369/JSST.2020.29.2.75
pISSN 1225-5475/eISSN 2093-7563

Flicker-free Visible Light Communication Using Three-level RZ Modulation

Seong-Ho Lee[+]

Abstract

We introduce a new visible light communication (VLC) method in which three-level return-to-zero (RZ) modulation is used for flicker-free transmission. In the VLC transmitter, the three-level RZ modulation ensures that the average optical power is constant; thus, a flicker-free light-emitting diode (LED) light is achieved. In the VLC receiver, a resistor–capacitor high-pass filter is used for generating spike signals, which are used for data recovery while eliminating the 120 Hz optical noise from adjacent lighting lamps. In transmission experiments, we applied this method for wireless transmission of an air quality sensor message using the visible light of an LED array. This configuration is useful for the construction of indoor wireless sensor networks for air pollution monitoring using LED lights.

Keywords: Visible light communication, Three-level RZ modulation, LED, Flicker-free, *RC*-HPF, Spike signal, Noise

1. INTRODUCTION

Light-emitting diodes (LEDs) are extensively used as the primary light source in various areas, such as indoor lighting in offices and homes, security lighting for streets, and car lighting. When compared to the traditional fluorescent lamps or incandescent lamps, LEDs demonstrate several advantages, including high power efficiency, high mechanical strength, and small size. In addition, the illumination of LEDs can be easily controlled by changing the injection current and the response is significantly fast, i.e., within a few microseconds. By utilizing the intrinsic high-speed response characteristics of the LEDs, visible light communication (VLC) technology was developed, in which communication and lighting functions are performed simultaneously [1-6]. In VLC, an LED light is generally used as the carrier for wireless data transmission for short distances and the signal light from the transmitter is directly detected by the photodetector through free space. Visible light and radio frequency do not interfere with each other; thus, VLC can be a good transmission method in places where electromagnetic interference should be avoided or where high security is required to prevent eavesdropping [7].

Because the LED light is used for both illumination and communication in VLC, the systems should be designed such that illumination and communication do not affect each other. For example, the LED illumination can be changed unintentionally during communication owing to the variation in the average optical power of the LED. This phenomenon may result in LED light flicker, which is a very unstable lighting condition; thus, appropriate methods should be provided to eliminate LED flicker. In the VLC receiver, the photodiodes (PDs) may be exposed to unwanted light from adjacent lighting lamps while it receives the signal from the transmitter. Incandescent lamps, fluorescent lamps, or other LED lamps, which are powered by a 60 Hz power line, generally radiate an optical noise of 120 Hz, which corresponds to twice the power-line frequency. Because the optical noise is also in the visible spectrum, it is detected by the VLC receiver. Consequently, the 120 Hz noise is induced in the VLC receiver while receiving the signal light transmitted from the VLC transmitter. If the optical noise intensity is not negligible, it may interfere with the signal and can cause errors during data transmission, especially in baseband VLC systems. Thus, a noise prevention method should also be considered in the system design. In baseband VLC systems, Manchester code modulation and pulse-position modulation are generally used for preventing LED flicker because they maintain the average optical power as constant in the transmitter. These schemes require an additional channel for clock transmission to recover the data in the receiver [5, 8].

Department of Electronics and IT Media Engineering, Seoul National University of Science and Technology, 232 Gongneung-ro, Nowon-gu, Seoul, 01811, Korea
[+]Corresponding author: shlee@seoultech.ac.kr
(Received :Oct. 16, 2019, Accepted : Feb. 04, 2020)

Subcarrier modulations, such as amplitude shift keying or frequency shift keying, have also been widely used as effective methods to prevent the flicker in the transmitter because the average optical power has to be maintained constant during data transmission [5]. The 120 Hz noise is easily cut off using a band-pass filter in the receiver. These subcarrier systems require additional electronic circuits for modulating and demodulating the subcarrier; thus, the system design may be more complex to implement than that of the baseband systems.

In this paper, we introduce a new baseband transmission method in which three-level return-to-zero (RZ) modulation is used for preventing the flicker of LED lights; further, spike detection is used for the 120 Hz noise prevention. In the VLC transmitter, three field-effect transistors (FETs) are used for supplying LED current, in which two FETs are for the three-level LED modulation and another FET is for controlling the DC optical power. The total current of the two FETs constitute a three-level RZ modulation signal, in which the average optical power of the LED light is maintained constant; thus, the flicker is eliminated. In the VLC receiver, a resistor–capacitor high-pass filter (*RC*-HPF) was used for generating spike signals while eliminating the 120 Hz noise from adjacent lighting lamps. The spike signal was used for recovering the transmitted non-RZ (NRZ) data.

This method is very simple and effective to use because this system does not require a separate clock channel or carrier for preventing flicker and noise intrusion. In experiments, as an application example of this method, we used the LED light for indoor wireless transmission of air quality sensor data to a mobile phone. This configuration can be widely utilized for constructing various sensor networks, such as gas, dust, temperature, and humidity sensors, using the LED lights in intelligent buildings.

2. SYSTEM CONFIGURATION

2.1 Visible light communication (VLC) transmitter

In the VLC transmitter, three-level RZ modulation is used for flicker-free transmission. Fig. 1 schematically shows the configuration of the VLC transmitter.

The VLC transmitter is composed of a microprocessor, three FETs, and an LED array. The input signals to the VLC transmitter are codes based on the American Standard Code for Information Interchange (ASCII) in NRZ waveforms. When the input signal is applied to the input port, the microprocessor outputs two voltages

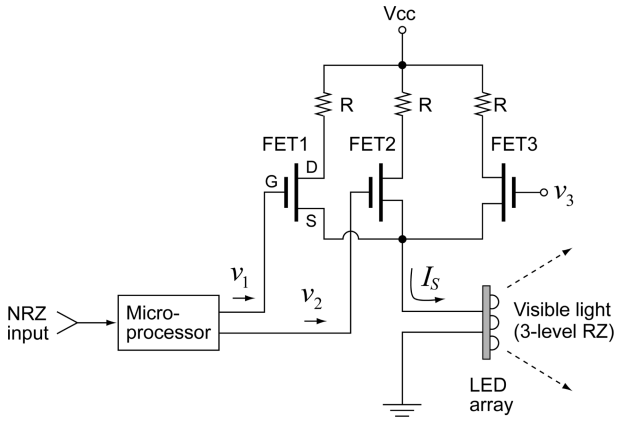

Fig. 1. Configuration of the visible light communication (VLC) transmitter.

(v_1 and v_2), which are applied to the gates of FET1 and FET2, respectively. The source currents of FET1 and FET2 are proportional to their gate voltages v_1 and v_2, respectively. The two source currents are added at the common source point and the total current (I_S) flows to the LED array. The output light of the LED array is proportional to the sum of the two source currents and its intensity constitutes a three-level RZ waveform. FET3 is not directly concerned with the RZ modulation; it is used for illumination control by changing the DC gate voltage v_3.

The three-level RZ waveform generation process is explained in Fig. 2. Fig. 2(a) is an arbitrary ASCII code character in NRZ waveform. For convenience, we used an 8-bit character "V" with a start bit and a stop bit. This format is generally used in universal asynchronous receiver and transmitter (UART) communication between computers or microprocessors. The microprocessor in the transmitter generates v_1 and v_2 signals corresponding to the NRZ input character, as shown in Figs. 2(b) and 2(c), respectively. When the NRZ input bit is in "high (H)" state, v_1 is in "H" state only during the former half part of the bit time (t_B) and in "low (L)" state elsewhere, as shown in Fig. 2(b). When the NRZ input bit is in "H" state, v_2 is in "L" state only during the latter half part of the bit time, and in "H" state elsewhere, as shown in Fig. 2 (c). The sum of the two source currents of FET1 and FET2 is proportional to the sum of the two voltages v_1 and v_2; thus, the LED light constitutes a three-level RZ waveform as shown in Fig. 2(d). The optical power densities at the lowest, medium, and highest levels are designated as 0, P_0, $2P_0$, respectively, in Fig. 2(d).

When the input NRZ bit is in "H" state, the average optical power in the three-level RZ modulated light can be calculated as follows.

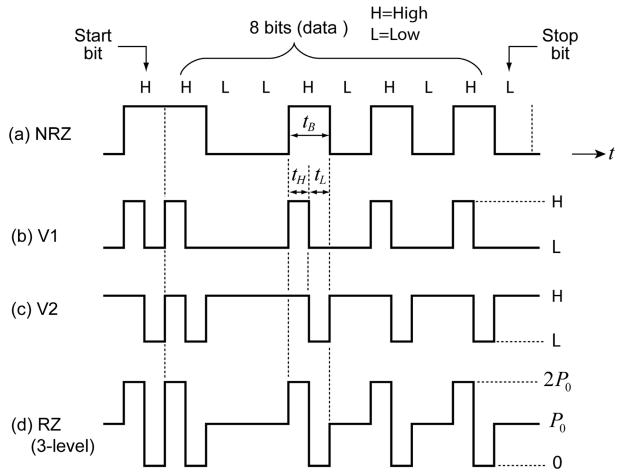

Fig. 2. Three-level return-to-zero (RZ) signal generation: (a) non-RZ (NRZ) input, (b) voltage v_1, (c) voltage v_2, and (d) three-level RZ output.

$$P_{avg}(H) = \frac{1}{t_B}\int_{t=0}^{t_B} P(t)\,dt = \frac{1}{t_B}(2P_0 \times t_H)$$
$$= \frac{1}{t_B}(2P_0 \times 0.5t_B) = P_0 \quad (1)$$

Here, t_B is a one-bit time of the NRZ input, $t_H = 0.5t_B$, which is the duration of the highest level in the three-level RZ modulated light, and P_0 is the optical power density at the medium level. When the input NRZ bit is in "L" state, the average optical power in the three-level RZ modulated light is constant at the medium level P_0, as shown in Fig. 2(d), that is

$$P_{avg}(L) = P_0 \quad (2)$$

Thus, the average optical power is constant at the medium level P_0 independent of the bit state. Consequently, the average optical power of the three-level RZ modulated light achieves constant illumination without LED flicker.

To observe the conversion process from NRZ input to three-level RZ waveform in the VLC transmitter, a character "V" was transmitted repeatedly; we observed the corresponding signal waveforms in the transmitter. Fig. 3 shows the voltage waveforms that were observed with an oscilloscope.

Fig. 3(a) is the voltage waveform of a character "V" in 9.6 kbps UART format. The ASCII code of character "V" is "01010110." When the least significant bit is sent first, the bit sequence from left to right becomes "01101010." Further, a start bit "0" and a stop bit "1" are added before and after the character, respectively. Thus, the waveform of the character "V" becomes a 10-bit signal, i.e., "0011010101."

In the UART transmission using Recommended Standard 232

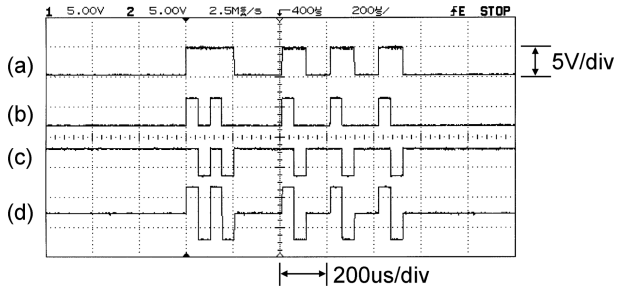

Fig. 3. Waveforms observed in VLC transmitter: (a) input NRZ waveform, (b) voltage v_1, (c) voltage v_2, and (d) three-level RZ waveform.

(RS-232), "H" is assigned to a "0" bit and "L" to a "1" bit. Consequently, the NRZ waveform of the character "V" becomes "HHLLHLHLHL," as shown in Fig. 3(a). Figs. 3(b) and 3(c) correspond to the voltages v_1 and v_2, which were applied to the gates of FET1 and FET2, respectively. Fig. 3(d) indicates the voltage at the common source point where the two FET source currents were added. The total current flowed into the LED array and three-level RZ visible light was radiated into the free space.

In the VLC transmitter, we used an ATmega8 microprocessor, three IRF540 FETs, and an LED array, which was fabricated in the form of a 2 × 3 planar array using six 1 W white-light LEDs.

2.2 VLC receiver

The VLC receiver detects the visible light and recovers the data sent from the VLC transmitter. The schematic diagram of the VLC receiver is shown in Fig. 4.

The VLC receiver is composed of a PD, amplifiers, an *RC*-HPF, and a microprocessor. The PD converts the input light to photocurrent, which flows through the load resistance R_L. The PD voltage across R_L is amplified and passed through the *RC*-HPF.

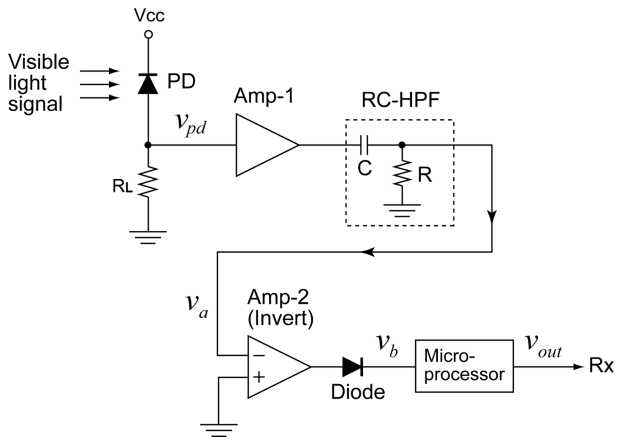

Fig. 4. Configuration of the VLC receiver.

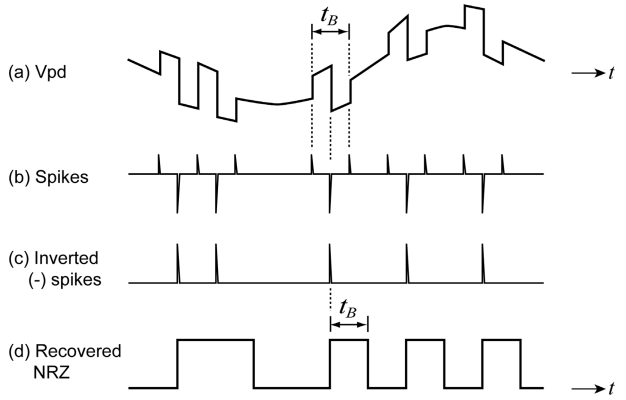

Fig. 5. Signal recovery process using spikes: (a) photodiode (PD) voltage, (b) spikes at resistor–capacitor high-pass filter (RC-HPF) output, (c) inverted negative spikes, and (d) regenerated NRZ waveform.

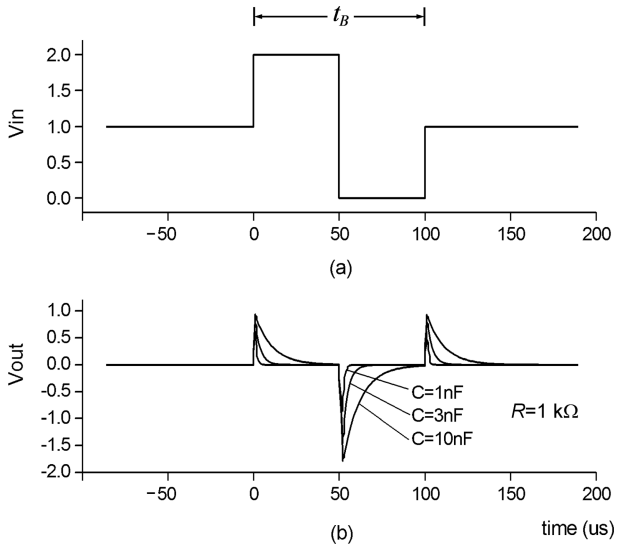

Fig. 6. Simulation of *RC*-HPF: (a) three-level RZ signal input voltage and (b) output spikes.

The *RC*-HPF cuts off the 120 Hz noise and outputs spike signals at the rising and falling edges of the three-level RZ signal. The microprocessor regenerates the NRZ data using the spikes from the *RC*-HPF output. The data recovery process in the VLC receiver is illustrated in Fig. 5.

In environments where the 120 Hz optical noise from adjacent lighting lamps is incident on the PD, the three-level RZ signal is mixed with optical noise and the PD voltage is as illustrated in Fig. 5(a). When the PD voltage passes through the *RC*-HPF, the 120 Hz noise disappears, and voltage spikes appear at the *RC*-HPF output, as shown in Fig. 5(b). The positive spikes appear at the rising edges and the negative spikes at the falling edges of the three-level RZ signal. When the NRZ bit in the transmitter is in "H" state, two positive spikes and one negative spike appear in a one-bit time (t_B). When the NRZ bit in the transmitter is in "L" state, no spike appears. Thus, we can use the negative spikes for regenerating the NRZ data sent from the transmitter.

Fig. 5(c) illustrates the inverted negative spikes that appear at the diode output after the inverted amplifier. These inverted negative spikes are applied to the interrupt port of a microprocessor. For each negative spike, the microprocessor generates a NRZ "H" bit whose duration corresponds to the one-bit time (t_B) of the NRZ data. Thus, the NRZ data is regenerated in the receiver, as shown in Fig. 5(d). The NRZ waveform regenerated in the receiver has the same shape as that in the transmitter; further, a time delay of half a bit time ($t_B/2$) exists between the transmitter and the receiver.

To verify the operation of the *RC*-HPF in the VLC receiver, we simulated its response to the three-level RZ signal and the 120 Hz noise using the PSpice program. The three-level RZ voltage at the input of the *RC*-HPF for one "H" bit of the NRZ data can be expressed as follows.

$$v_{RZ}(t) = V_S\left[U(t) - 2U(t - 0.5t_B) + U(t - t_B)\right] \tag{3}$$

Here, Vs is voltage amplitude, $U(t)$ is the step function, and t_B is the one-bit time of the NRZ data in the VLC transmitter. Fig. 6 shows the simulated voltage of the *RC*-HPF. In the simulation, we used unit amplitude, that is $V_S = 1$; the bit time $t_B = 100$ μs; the resistance of the *RC*-HPF was set to $R = 1$ kΩ; moreover, the capacitor C was used as a parameter. Fig. 6 shows the simulation result.

Figs. 6(a) and 6(b) are the three-level RZ input and output voltage waveforms of the *RC*-HPF, respectively. Positive and negative spikes appear at the rising and falling edges of the three-level RZ voltage, respectively. The negative spike appears once only at each "H" bit of NRZ data and it is used for recovering the NRZ bit sequence sent from the transmitter. The *RC*-HPF response to the 120 Hz noise was also simulated using the PSpice program. The 120 Hz noise can be expressed approximately as presented below.

$$v_{Noise}(t) = V_N \cos(2\pi \times 120t) \tag{4}$$

Here, V_N is the noise voltage amplitude. In the simulation, we used unit amplitude, that is $V_N = 1$; moreover, the resistance of the *RC*-HPF was set to $R = 1$ kΩ, and the capacitor C was used as the parameter. Fig. 7 shows the simulation result.

Figs. 7(a) and 7(b) are the 120 Hz noise input and output voltage waveforms of the *RC*-HPF, respectively. As seen in Fig. 7

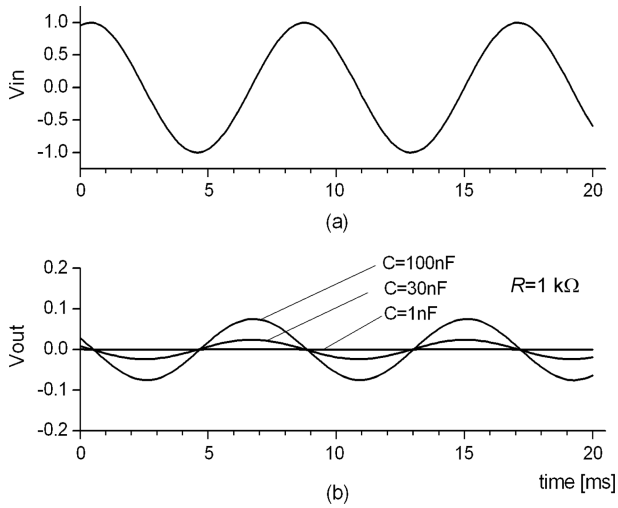

Fig. 7. Simulation of *RC*-HPF: (a) input noise voltage and (b) output noise voltage.

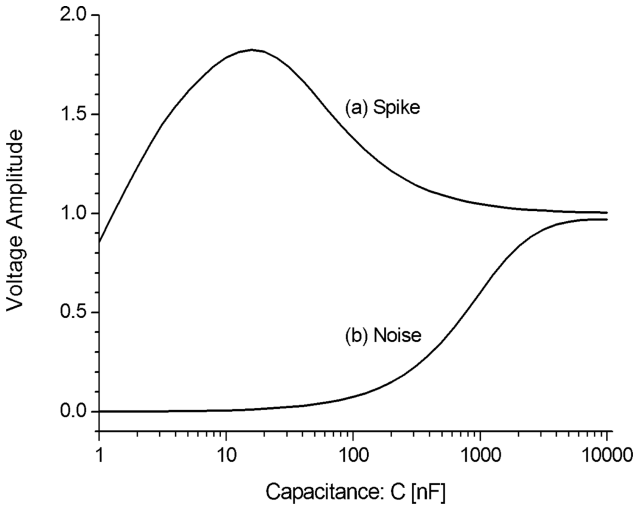

Fig. 8. Spike and noise amplitude variations according to the capacitance at the *RC*-HPF output.

(b), the noise output voltage decreased as the capacitance decreased. For the capacitance smaller than 10 nF, the output noise decreased to a value 1/100 times lower than the input. Fig. 8 shows the amplitude variations of the negative spikes and the 120 Hz noise at the *RC*-HPF output corresponding to the changes in capacitance. In the simulation, the resistance of the *RC*-HPF was fixed at R = 1 kΩ and the capacitance C was varied as an independent variable.

In Fig. 8, the spike amplitude shows the maximum value at a range of approximately 10 nF to 30 nF and the noise amplitude decreased monotonically as the capacitance reduced. In transmission experiments, we used C = 10 nF and R = 1 kΩ for the *RC*-HPF to obtain the maximum spike amplitude while suppressing the noise.

To observe the behavior of the VLC receiver, a character "V" was transmitted repeatedly and the voltage waveforms in the VLC receiver were observed. Fig. 9 shows the voltage waveforms observed using the oscilloscope.

Fig. 9(a) shows the PD voltage when it received the three-level RZ signals while exposed to the 120 Hz noise. The large slope in PD voltage is due to the 120 Hz noise light. The RZ signal peak-to-peak amplitude was approximately 240 mV and the noise amplitude was approximately 250 mV. This is a situation where the noise strength is not negligible when compared to the signal.

Fig. 9(b) illustrates the positive and negative spikes that appeared at the *RC*-HPF output. When these spikes were applied to an inverted amplifier and a diode, the positive spikes were cut off and only the inverted negative spikes appeared at the diode output. The inverted negative spikes have positive voltages as

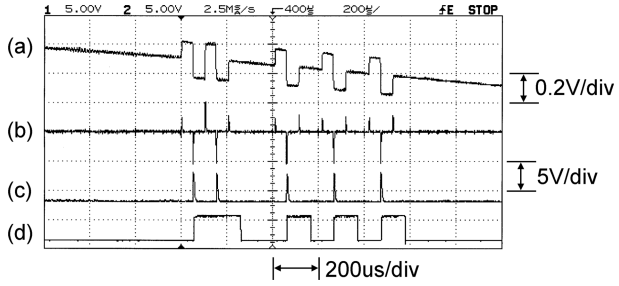

Fig. 9. Waveforms observed in VLC receiver: (a) PD voltage, (b) spikes at *RC*-HPF output, (c) the inverted negative spikes, and (d) the regenerated NRZ waveform.

shown in Fig. 9(c). These inverted negative spikes were applied to the interrupt port of the microprocessor. The microprocessor generated a rectangular pulse with a width of 104 μs per spike, which corresponds to the one-bit time in a 9.6 kbps UART signal. Consequently, the NRZ data was regenerated at the output of the microprocessor as shown in Fig. 9(d). This signal is in the same shape as the NRZ ASCII code sent from the VLC transmitter, which was shown in Fig. 3(a). The regenerated NRZ waveform in the receiver had a time delay of approximately 52 μs when compared to that in the transmitter. The time delay corresponds to half of the bit time of the NRZ data (t_B/2). This time delay appears because the negative spikes are generated at the half point of the NRZ "H" bit by the falling edge of the three-level RZ signal.

In the VLC receiver, we used a PIN PD, SFH-203, which has a current sensitivity of 0.6 A/W, sensitive area of 1 mm^2, rise time of approximately 100 ns with a load resistance of 1 kΩ. The resistance and capacitance of the *RC*-HPF were R = 1 kΩ, C = 10 nF, respectively; further, the cut-off frequency of the *RC*-HPF was

approximately 16 kHz. For Amp-1 and Amp-2 in the receiver, we used OPA228 operational amplifiers, and the microprocessor used was an ATmega8.

3. TRANSMISSION EXPERIMENT

The transmission method using the three-level RZ modulation and spike detection is effective in constructing a flicker-free VLC system and suppressing the 120 Hz noise from adjacent lighting lamps. We used this method for transmitting the message of an air quality sensor using LED lights. An air quality sensor detects the air pollution owing to the harmful gases, such as carbon monoxide, ammonia, and smoke of cigarettes. This configuration shows that the LED lamps can have additional functions, such as wireless sensor nodes, when it is coupled with various sensors. Fig. 10 is the experimental setup for transmitting the air quality sensor data to a mobile phone.

The air quality sensor, ZP01-MP503, outputs two voltages (Vs_1, Vs_2) corresponding to four types of air pollution states: clean (0, 0), light pollution (0, 5 V), moderate pollution (5 V, 0), and severe pollution (5 V, 5 V) [9]. The microprocessor in the transmitter reads the two voltages and modulates the LED array with the characters describing the air pollution state. The VLC transmitter, LED array, and air quality sensor were installed near the ceiling of the laboratory. The LED array was used simultaneously as indoor lighting lamp and as a VLC source. The VLC receiver was installed on a table and the distance from the transmitter was approximately 1.5 m. The visible light from the LED array was detected by the PD, and the NRZ data was recovered in the receiver circuit, and then sent to a mobile phone through a serial-to-USB converter.

When a character string “air-sensor: clean \r\n” was sent by the VLC transmitter, we observed the signal waveforms in the VLC receiver using an oscilloscope. Fig. 11 shows the observed voltage waveforms.

Fig. 11(a) illustrates the PD voltage waveform in the receiver in which the three-level RZ signal is mixed with the 120 Hz noise from adjacent lighting lamps. By using the *RC*-HPF the 120 Hz noise was eliminated; further, Fig. 11(b) illustrates the inverted negative spikes appearing at the diode output of the VLC receiver. Fig. 11(c) shows the recovered NRZ waveforms corresponding to the first five characters of the character string from the VLC transmitter.

The recovered NRZ signal was transferred to a mobile phone through a serial-to-USB converter. The mobile phone does not use RS-232 standard; thus, the NRZ voltage was inverted before it was applied to the mobile phone. Fig. 11(d) illustrates the inverted NRZ waveform in which “H” voltage denotes “1” and “L” is “0.” The inverted NRZ waveform was applied to the USB input port of a mobile phone through a serial-to-USB converter. Fig. 12

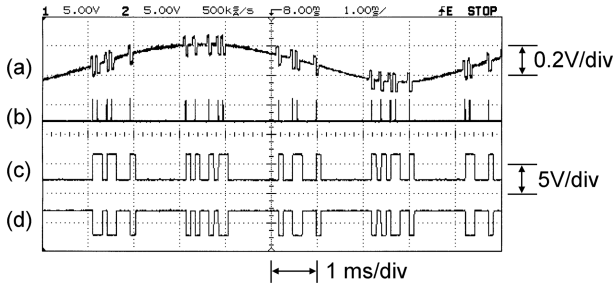

Fig. 11. Waveforms observed in the VLC receiver: (a) PD voltage, (b) inverted negative spikes, (c) recovered NRZ signal, and (d) inverted NRZ signal transmitted to a mobile phone.

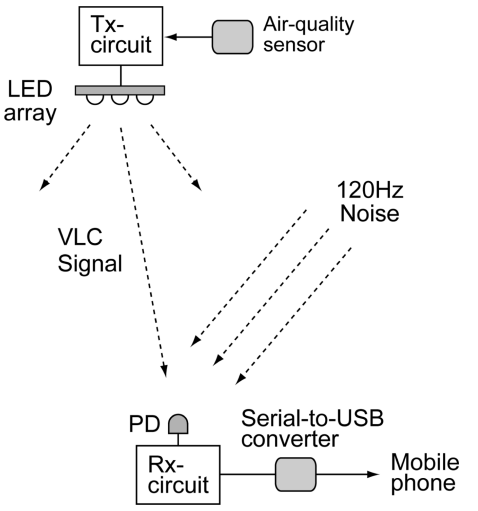

Fig. 10. Experimental VLC setup using three-level RZ modulation and spike detection.

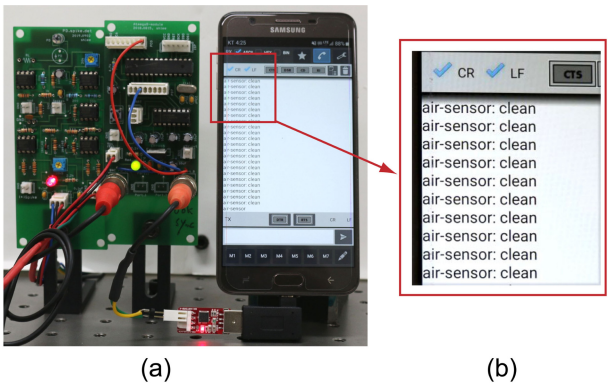

Fig. 12. Characters displayed on a mobile phone: (a) mobile phone screen and (b) characters displayed on the screen.

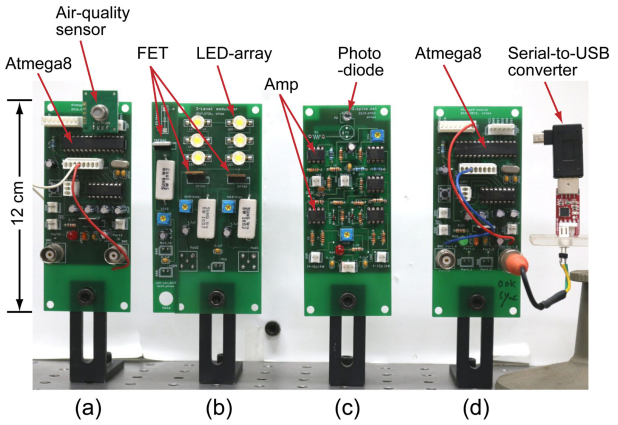

Fig. 13. Circuit boards used in the experiments: (a) microprocessor and air quality sensor, (b) FETs and light-emitting diode array, (c) the PD and amplifiers, and (d) microprocessor and serial-to-USB converter.

shows the characters displayed on the screen of the mobile phone.

The characters "air-sensor: clean" sent from the VLC transmitter were displayed on the mobile phone screen. The two characters "\r" (carriage return) and "\n" (line feed) did not appear on the screen because they are special characters for position control. Fig. 13 shows the circuit boards used in experiments.

Figs. 13(a) and 13(b) show the circuit boards used in the VLC transmitter; Figs. 13(c) and 13(d) show the circuit boards used in the receiver. Fig. 13(a) shows the microprocessor ATmega8 and the air quality sensor ZP01-MP503. Fig. 13(b) illustrates the 2 × 3 LED array and its current driving circuit using three IRF540 FETs. Fig. 13(c) shows the PIN PD, SFH-203, and OPA228 amplifiers in the receiver circuit. Fig. 13(d) shows the microprocessor ATmega8 and the serial-to-USB converter used in the receiver.

4. CONCLUSION

In this paper, we developed a new VLC transmission method for preventing the LED flicker in the transmitter and for eliminating the 120 Hz noise in the receiver. In the transmitter, three-level RZ modulation was used to maintain the average optical power of the LED light at a constant value. The three-level RZ waveform was generated using two FETs, which were parallel connected to each other. In the receiver, an *RC*-HPF was used to generate spikes while cutting off the 120 Hz noise. Among the positive and negative spikes, which appeared at the rising and falling edges, respectively, the negative spikes were inverted and used for regenerating the transmitted NRZ data. This configuration is significantly easy to implement because it does not require a subcarrier or an additional clock transmission for flicker prevention or adjacent 120 Hz noise suppression.

As an application example, we used the LED light for the indoor wireless transmission of an air quality sensor message to a mobile phone through the VLC receiver. This experiment demonstrated that an LED lamp can be simultaneously used as an illumination source and a wireless air-sensing node when it is coupled with an air quality sensor. This configuration is useful in constructing indoor air control systems, where each LED lamp operates as an individual sensing node from its high positions near the ceiling in factories, offices, subways, or hospitals, where real-time air condition monitoring is required for human safety.

ACKNOWLEDGMENT

This study was supported by the Research Program funded by the SeoulTech (Seoul National University of Science and Technology).

REFERENCES

[1] X. Ma, K. J. Lee, and K. S. Lee, "Appropriate modulation scheme for visible light communication systems considering illumination", *Electron. Lett.*, Vol. 48, No. 18, pp. 1137-1139, 2012.

[2] S. Rajagopal, R. D. Roberts, and S. K. Lim, "IEEE 802.15.7 visible light communication: modulation schemes and dimming support", *IEEE Commun. Mag.*, Vol. 50, No. 3, pp. 72-82, 2012.

[3] Y. K. Cheong, X. W. Ng, and W. Y. Chung, "Hazardless biomedical sensing data transmission using VLC", *IEEE Sens. J.*, Vol. 13, No. 9, pp. 3347-3348, 2013.

[4] S. H. Lee, "A passive transponder for visible light identification using a solar cell", *IEEE Sens. J.*, Vol. 15, No. 10, pp. 5398-5403, 2015.

[5] C. Yao, Z. Guo, G. Long, and H. Zhang, "Performance Comparison among ASK, FSK and DPSK in Visible Light Communication", *Opt. Photonics J.*, Vol. 6, pp. 150-154, 2016.

[6] A. M. Cailean and M. Dimian, "Current Challenges for Visible Light Communications Usage in Vehicle Applications: A Survey", *IEEE Commun. Surv. Tutor.*, Vol. 19, No. 4, pp. 2681-2703, 2017.

[7] V. P. Rachim, Y. Jiang, H. S. Lee, and W. Y. Chung, "Demonstration of long-distance hazard-free wearable EEG monitoring system using mobile phone visible light communication", *Opt. Express*, Vol. 25, No. 2, pp. 713-719, 2017.

[8] S. H. Lee, "Illumination control of LEDs in visible light communication using Manchester code transmission", *J. Sens. Sci. Technol.*, Vol. 25, No. 5, pp. 303-309, 2016.

[9] Zhengzhou Winsen Electronics Technology, *Air quality detection module user's manual*, p.5, 2014.